Arabian Journal of Chemistry (2019) xxx, xxx–xxx

King Saud University

Arabian Journal of Chemistry

www.ksu.edu.sa
www.sciencedirect.com

ORIGINAL ARTICLE

Low-cost preparation method of well dispersed gold nanoparticles on reduced graphene oxide and electrocatalytic stability in PEM fuel cell

Adriana Marinoiu [a,*], Mircea Raceanu [a], Mindaugas Andrulevicius [b], Asta Tamuleviciene [b], Tomas Tamulevicius [b], Simona Nica [c], Daniela Bala [d], Mihai Varlam [a]

[a] *RD Institute for Cryogenics and Isotopic Technologies-ICSI, 4 Uzinei St., 240050 Rm Valcea, Romania*
[b] *Institute of Materials Science, Kaunas University of Technology, K. Baršausko str. 59, Kaunas LT-51423, Lithuania*
[c] *Romanian Academy, "C. D. Nenitzescu" Institute of Organic Chemistry Splaiul Independentei 202 B, 060023 Bucharest, Romania*
[d] *Department of Physical Chemistry, Faculty of Chemistry, University of Bucharest, Romania*

Received 20 October 2018; accepted 20 December 2018

KEYWORDS

Graphene;
Reduced graphene oxide;
Au nanoparticles;
PEMFC

Abstract A facile and feasible protocol for synthesis of functionalized reduced graphene oxide decorated with gold nanoparticles (AuNP/rGO) in mild reaction conditions has been successfully developed. Starting from graphite, the following synthesis routes were developed: (1) preparation of graphite oxide; (2) graphene oxide (GO) functionalized with a compatible polymer; (3) reduced graphene oxide decorated with gold nanoparticles (final compound). The surface morphology of as-prepared AuNP/rGO was investigated using scanning electron microscopy (SEM) and specific surface area was determined using BET method, while structural properties were investigated using Raman scattering spectroscopy, X-Ray photoelectron spectroscopy (XPS), Fourier-transform infrared spectroscopy (FTIR). This comprehensive study demonstrated the simultaneous reduction of GO and the achievement of Au nanoparticles dispersed on graphene sheets. An ORR catalytic system containing prepared AuNP/rGO was developed, and electrochemical measurements were performed. Firstly, the *ex-situ* electrochemical performances of AuNP/rGO-modified carbon electrode were investigated using cyclic voltammetry. Secondly, the *in-situ* electrochemical evaluation were carried out as application in real PEM fuel cell and analyzed as comparison commercial Pt/C *versus* developed ORR catalytic system. The *in-situ* CV results showed that the oxidation and reduction peaks corresponding to hydrogen adsorption/desorption decreased differently,

* Corresponding author.
E-mail address: adriana.marinoiu@icsi.ro (A. Marinoiu).
Peer review under responsibility of King Saud University.

Production and hosting by Elsevier

https://doi.org/10.1016/j.arabjc.2018.12.009

Please cite this article in press as: Marinoiu, A. et al., Low-cost preparation method of well dispersed gold nanoparticles on reduced graphene oxide and electrocatalytic stability in PEM fuel cell. Arabian Journal of Chemistry (2019), https://doi.org/10.1016/j.arabjc.2018.12.009

indicating that a decrease of electrochemical surface area occurs for both cases, more visible for commercial catalyst. The cathode made with AuNP/rGO developed in this work, tested in hydrogen-air PEMFC, had a power density of 0.59 W cm $^{-2}$ at 0.6 V, a meaningful voltage for fuel cells operation, comparable with that of a commercial Pt-based cathode tested under identical conditions, but a superior electrochemical stability. The results confirmed that the developed AuNP/rGO nanoparticles could be valuable alternative ORR nanostructured electrodes.

1. Introduction

The intriguing characteristics of graphene, such as unique electrical, mechanical, physical and chemical properties have conferred a merited and recognized interest for this material, mainly due to the extremely high carrier mobility, quantum Hall effect or tunable work function, making it an attractive component for the fabrication of electronic devices. Graphene and also its various related materials demonstrated also interesting advantages in electrochemical devices such as fuel cells.

A highly desirable and long awaited large-scale commercialization of fuel cells is still restricted and conditioned widely by the slow kinetics of the cathodic oxygen reduction reaction (ORR). Commonly, Pt-based nanomaterials are used as best active electrocatalysts for both anode and cathode in proton exchange membrane fuel cells (PEMFCs) (Yaldagard et al., 2013; Meier et al., 2014; Hellman and Van den Hoed, 2007; Gasteiger et al., 2005).

However in the last few years Pt nanomaterial has begun to appear more and more outdated due to some unsolvable problems to date, such as susceptibility to the crossover effect, high cost together with its limited resources. Therefore, aiming to minimize the usage of Pt, the development of alternative efficient electrocatalysts for ORR at the cathode in fuel cells has generated a great interest. Moreover, the long term stability of the ORR catalyst has been already recognized as the key to overall system durability.

To replace platinum-based catalysts, the improved catalysts for ORR must meet the following three criteria: a specific volumetric activity in comparison with Pt-based catalysts in order to meet the US department of energy (DOE)'s 2015 target, excellent mass-transport properties and high durability. While the first two criteria have demonstrated recently some relevant scientific breakthroughs at a level sufficient for practical applications, the third criteria is still a major challenge. To date, ORR cathodes have not shown yet sufficient electrochemical stability for polymer electrolyte membrane fuel cells operation.

The strong dependence for the operation conditions makes sense to include the anticipated degradation as mandatory durability test. Therefore, the durability is still a critical issue to cope with PEMFC field in order to achieve a large commercialization and a real competition with combustion engines. In this respect, the lifetime of automotive FC devices drop in performance manly due to chemical and mechanical degradation. Relevant research focused on the degradation of FC, ranging from the detailed electrochemical modeling to empirical work on accelerated ageing testing, have been recently reported.

The accurate control of the electrical transport is considered critical for the development of cathodic electrocatalysts. The graphene oxide (GO), a 2D structured material with a large surface area, is considered an alternative to graphene, due to its low cost, production scalability or good compatibility. The structural and electronic properties of graphene can be modified by chemical adsorption of metal atoms or by incorporation of metal atoms into the lattice. The surface decoration using gas molecules or metal nanoparticles can tune the band structure of graphene. Thus the presence of defects in graphene is speculated to achieve new functionalities. The graphene doping with metal atoms has received great attention mainly in respect to the transition metal atoms bound on graphene or embedded in single and double vacancies (Liu et al., 2014; Hsieh et al., 2013; Shao et al., 2010; Cheng et al., 2014). Both n- and p-type conductivities can be obtained by selecting metal dopants, and the carrier concentration can be controlled by the quantity of deposited metal. For example, several transition metals with different work functions, such as Ti, Fe, Cu, Ag, Au, and Pt, have been used for graphene band modulation (Tang et al., 2011).

A suitable ORR catalyst has to offer both catalytic activity and selectivity, but also has to able to resist in the harsh chemical environment during long-term PEMFC operational conditions, such as presence of oxidant, reactive radicals, strong acidic conditions at low pH, rapid potential fluctuations. The specific environment from the PEMFC operation demands limited alternatives for materials that can be used as ORR electrocatalysts. Only three elements with bulk nominal dissolution potential U_{diss} higher than the FC operating potential of ~0.8–1.0 V (vs the standard hydrogen electrode SHE) are recommended, namely: Ir, Pt, and Au, having U_{diss} of 1.16, 1.18, and 1.5 V (vs. SHE), respectively. Actually, as been demonstrated, in real FC application the problem is more severe. For example, in strong acidic medium for pH < 1, the Pt dissolution potential affords an on set electrode potential of 0.65 V, which is much lower than the operating potential of an efficient FC (Stolbov and Alcántara Ortigoza, 2015).

Despite of a known less catalytic activity of Au in comparison to Pt regarding the FC application, we propose to develop an ORR electrocatalytic system containing commercial Pt/C and AuNP, whose fabrication is going to be discussed later.

The redistribution of electronic states in graphene lattice could make the metal dopant atom more active toward ORR and Au might be the best option due to its electrochemical stability in acidic reaction, i.e. typical operating conditions of FC. Taking into account that the gold is the most stable metal against dissolution, recently few attempts were performed in order to incorporate Au atoms into the carbon vacancies created in graphene layers, and investigate its performance as ORR electrocatalysts. It has been indicated that Au is strongly

Please cite this article in press as: Marinoiu, A. et al., Low-cost preparation method of well dispersed gold nanoparticles on reduced graphene oxide and electrocatalytic stability in PEM fuel cell. Arabian Journal of Chemistry (2019), https://doi.org/10.1016/j.arabjc.2018.12.009

bound to the di-vacancy (DV) and its diffusion barriers are high (~4 eV), which ensures the stability of the catalytic system. Au-atom dopants are incorporated into one of the most thermodynamically stable carbon vacancies created in graphene: the 5-8-5 DV, so the Au-doped graphene could be fully considered a highly stable and active electrocatalysts for ORR (Stolbov and Alcántara Ortigoza, 2015).

More precisely, gold nanoparticles have received remarkable attention as catalytic nanoparticles due to its physical and chemical properties, such as easily controllable size distribution, long-term stability, and superior conductivity (Likai et al., 2016; Qiannan et al., 2016; Tang et al., 2018). However, there is still a significant challenge in controlling the uniformity of graphene surface decoration with metal nanoparticle and especially the strength of the attachment between the organic and the inorganic components. Despite bulk gold being chemically inert, gold nanoparticles are surprisingly catalytically effective for ORR without the drawbacks associated to platinum. Actually, creating stable AuNP catalysts has proven problematic. Previous fabrication methods have produced catalysts with more or less regulates sizes. Meanwhile, efforts to produce stable catalysts for practical use were addressed.

On the other hand, Poly-diallyldimethylammoniumchloride (PDDA) has been used as cationic polyelectrolyte, due to the ability of adsorption on the graphene surface through $\pi-\pi$ and electrostatic interactions, acting as a stabilizer for controlled synthesis of Pt/graphene (Lei et al., 2013). The physical adsorption of PDDA, a positively charged polyelectrolyte with electron-retract ability on graphene could create net positive charge on carbon-atoms in the all-carbon graphene plane through the intermolecular charge transfer. Graphene nanosheets with negative charge can be easily functionalized by positively charged PDDA through the electrostatic interaction, which can increase the stability of graphene in solution. A key factor guaranteeing the feasibility of this system is that the resultant PDDA-functionalized/ adsorbed graphene possess enhanced electrocatalytic activities toward ORR (Wang et al., 2011; Borowiec et al., 2015). The Au loading density can be effectively adjusted by simply changing the ratio of PDDA to the Au precursor.

The proposed synthetic method is inexpensive, simple, rapid, requires low temperatures (close to room temperature). Starting material include extremely low cost material (graphite). The production of graphene oxide decorated with gold is currently achieved by graphene growth via chemical vapor deposition on a metallic surface, followed by transfer of the carbon layer on the oxide, by atomic layer and physical vapor deposition of the oxide on graphene or by carbon deposition on top of oxide surface. The mentioned methods involve some issues: they are costly, require complex procedures and can easily result in damage of the carbon network with substantial effects on the carrier mobility. Moreover, to the best of our knowledge, Au supported on reduced graphene oxide has not been reported as ORR catalyst in real-time PEMFC operation. In this paper we explored a low cost synthesis route of AuNP/rGO nanocomposites by in-situ co-reduction of GO and Au precursor in the presence of PDDA. The as-prepared sample was used in fabrication of a hybrid cathode and its electrochemical properties were investigated. The Au-based catalyst was added to the cathode layer, with the purpose of improving of electrocatalytic stability in real-time PEMFC operation conditions. The promising results may provide many potential applications for other electrochemical devices, in particular in PEMFC domain.

2. Experimental

2.1. Reagents and materials

Purified natural graphite (PMM7) with the following characteristics: C = min. 99.5 wt.%, ash = max. 0.5 wt.%, specific surface = 9 m^2/g (BET) was delivered by KOH–I-NOR Grafit S.R.O (Czech Republic). Chloroauric acid ($HAuCl_4 \cdot 3H_2O$, ≥49.0% Au basis), Poly-diallyldimethylammonium chloride (PDDA 20 wt.% in water solution, average molecular weight 200 000–350 000), phosphorus pentoxide (P_2O_5, 98%), hydrogen peroxide (H_2O_2 analytical grade, 30% aqueous solution), hydrochloric acid (HCl, 30%) and sodium carbonate (Na_2CO_3, 99.5% min) were purchased from Sigma-Aldrich. Potassium permanganate ($KMnO_4$ ACS, 99.0% min) and sulfuric acid (H_2SO_4, 99.8%) was procured from Alfa Aesar. Sodium borohydride ($NaBH_4$ 98 wt%) was purchased from Fluka. The water used was purified through a Millipore system (> 18.2 MΩ cm).

2.2. Preparation of AuNP/rGO nanocomposites

Fabrication of AuNP/rGO nanocomposites was performed step by step: (1) preparation of graphite oxide from graphite; (2) synthesis of graphene oxide; (3) functionalization of graphene oxide with PDDA as compatible polymer; (4) incorporation of precursor chloroauric acid leading to formation of reduced graphene oxide decorated with gold (AuNP/rGO).

2.2.1. Synthesis route for graphite oxide

The graphite oxide was obtained via a solution-based route, involving the chemical oxidation of graphite, as was reported in our earlier reports (Marinoiu et al., Marinoiu et al., 2017). Briefly, graphite flakes were mixed with concentrated H_2SO_4, $K_2S_2O_8$, P_2O_5, under stirring at room temperature. After heating up for 4 h at 80 °C, the mass was cooled in natural conditions. Potassium permanganate was added slowly at temperature below 10 °C, and the mixture was stirred in the ice bath for 1 h. The reaction mass was gradually heated to 50 °C and stirred in thermostatic bath for 6 h. Afterwards, the temperature was reduced to room temperature and hydrogen peroxide H_2O_2 was added until the solution turned to yellow. Then the solution was centrifuged (10,000 rpm for 1 h), and the supernatant was removed. The remaining solid material was washed several times alternating water and hydrochloric acid. After repeated separation procedures (washing and ultracentrifugation at 16,000 rpm for 30 min), the suspension was dried using two methods. One part of the product in the form of gel was dried by a freeze drying technique namely the lyophilization method. The obtained solid product was encoded *graphite oxide sample A*. This drying method was used in order to reduce the probability of formation of irreversible agglomerates and even restacking in graphite which is often obtained during the conventional drying process. Another part of the product was dried conventionally under vacuum at approx. 50 °C in air flow to constant weight (this sample was named *graphite oxide sample B*).

Please cite this article in press as: Marinoiu, A. et al., Low-cost preparation method of well dispersed gold nanoparticles on reduced graphene oxide and electrocatalytic stability in PEM fuel cell. Arabian Journal of Chemistry (2019), https://doi.org/10.1016/j.arabjc.2018.12.009

2.2.2. Preparation of graphene oxide

Graphite oxide samples (sample A and sample B) were dispersed in deionized water separately. The dispersion was firstly exfoliated for 1 h to form multi-layered graphene oxide by ultrasonication at 110 W/40 kHz at 30–40 °C. This pre-exfoliation step ensures a better uniformity of dispersion of graphite oxide and facilitates a more intimate contact with the binder introduced later on. The pH of dispersed gel was corrected to 9 with Na_2CO_3 and reaction mass was stirred for 1 h at the room temperature.

2.2.3. Functionalization of graphene oxide with PDDA

Adequate quantities of PDDA solution (0.5 mL sol. for 1 g GO) were introduced in order to prepare approximately 5.4 wt%). The exfoliation was continued by sonication for 1 h to 110 W and 40 kHz at 40 C. Afterwards, the reaction mass was separated by ultracentrifugation and the solid was washed out. The adsorption of PDDA made the surface of graphene positively charged, leading to a good dispersion via electrostatic rejection among individual graphene sheets, which are also solubilized by the adsorbed PDDA chains. In the absence of PDDA, the $NaBH_4$-reduced graphene could precipitate (Marinoiu et al.).

2.2.4. Preparation of reduced graphene oxide decorated with gold nanoparticles (AuNP/rGO)

The experimental procedure employs the preparation of Au-graphene nanosheets as follows. $HAuCl_4{\cdot}3H_2O$ (3 g) was added to the dispersed exfoliated mixture and the reaction mass was stirred more than 12 h at room temperature. Finally, a reaction mass with pH = 3 was obtained. In the reduction step, the final stage of protocol, the obtained Au colloidal solution was added to a fresh $NaBH_4$ solution at 80 °C and dosed under stirring in aprox. 2 h. $NaBH_4$ was used as the reducing agent instead of hydrazine to avoid the doping of graphene with nitrogen that could provide certain ORR activity which interfere with the intermolecular charge-transfer effect (Wang et al., 2011). Upon addition of $NaBH_4$, the color of the suspension changed from the yellow-brown of GO to black for graphene and doped graphene. The reaction mass was maintained at 80 °C for 4 h, cooled to room temperature and separated by decantation and ultracentrifugation. The separated solid was dried using the described methods specifically for each sample, then was re-dispersed by sonication in H_2SO_4 and mechanically stirred for 12 h at 120 °C. After cooling, the reaction mass was washed with distilled water to completely remove the SO_4^{2-} ions, filtered, washed with water and ethanol and dried again. The prepared samples were encoded AuNP/rGO_A and AuNP/rGO_B, in respect to used drying method involved in proposed protocol (lyophilization for sample A and conventional drying in oven for sample B).

2.3. Characterization methods

Structure of formed samples was investigated using Raman scattering spectroscopy. Raman scattering measurements were performed using a Raman microscope inVia (Renishaw). The excitation beam from a diode laser of 532 nm wavelength was focused on the sample using a 50× objective (NA = 0.75, Leica). Laser power at the sample surface was 1.75 mW, integration time was 10 s, signal was accumulated 1 time. The Raman Stokes signal was dispersed with a diffraction grating (2400 grooves/mm) and data was recorded using a Peltier cooled charge-coupled device (CCD) detector (1024 × 256 pixels). This system yields a spectral resolution of about 1 cm^{-1}. Silicon line was used to calibrate the Raman setup in both Raman wavenumber and spectral intensity. The surface of the prepared samples was checked employing field emission scanning electron microscope (FE-SEM) FEI Quanta 200 FEG. Theoretical resolution of the SEM at 30 kV accelerating voltage is 1.2 nm. X-ray photoelectron spectroscopy (XPS) analysis was carried out employing a Thermo Scientific ESCALAB 250Xi spectrometer. Monochromatic Al Kα radiation ($h\nu$ = 1486.6 eV) was used as an excitation source. The 40 eV and 20 eV pass energy values of a hemispherical electron energy analyzer were used for the survey and high resolution spectra acquisition, respectively. The energy scale of the system was calibrated with respect to Au $4f_{7/2}$, Ag $3d_{5/2}$ and Cu $2p_{3/2}$ peak positions. ESCALAB 250Xi Avantage software was used for the peak deconvolution and calculation of atomic concentration. All spectra were fitted using symmetrical peaks and 70:30 Gauss-Lorentz function ratio unless stated otherwise in the text. The specific surface areas of the samples were determined using the Brunauer-Emmett-Teller (BET) method by performing nitrogen sorption measurements using a Quantachrome Autosorb IQ equipment. Pore size distribution data was obtained from desorption branches of isotherm using Barrett-Joyner-Halenda (BJH) method. The adsorption and desorption experiments were done at 77 K after initial pretreatment of the samples by degassing at 115 °C for 8 h. IR transmittance spectra were recorded on Bruker Tensor 37 spectrometer, in the 400–4000 cm^{-1} range using KBr pellets.

2.4. Electrode preparation and electrochemical measurements

The modified carbon paste electrodes were prepared by mixing graphite powder with paraffin oil with the ratio of 3:2 (w/w). Both components were mixed by hand for 40 min in a mortar until a consistent uniformly wetted paste was obtained, following our reported protocol (Marinoiu et al.). The obtained paste was placed into a 1.0 mL volume plastic syringe. The electrical contact was assured by a copper wire that was inserted into the back of the graphite paste. When it was necessary, a renew surface was obtained by pushing a small excess of the paste out of the tube and polishing it with a filter paper. The modified electrodes were prepared by mixing certain amounts of carbon paste with graphene oxide or gold doped reduced graphene oxide in ratio of 1% AuNP/rGO. Thus, four electrodes were prepared: (i) carbon paste electrode (CPE), (ii) graphene oxide modified carbon paste electrode (denoted by GO), (iii) two of gold-dopped reduced graphene oxide (denoted by AuNP/rGO_A and AuNP/rGO_B). The surface of all electrodes was smoothed by polishing on a piece of weighing paper. All electrodes were kept in distilled water before and after electrochemical measurements. Electrochemical measurements were carried out on a potentiostat galvanostat system AutoLabPGStat 12, controlled by general purpose electrochemical system (GPES), electrochemical interface for Windows (version 4.9.007). Three electrodes in one compartment cell (10 mL) were used in all experiments. A glassy carbon electrode (Metrohm, 3 mm in diameter) and prepared electrodes served

Please cite this article in press as: Marinoiu, A. et al., Low-cost preparation method of well dispersed gold nanoparticles on reduced graphene oxide and electrocatalytic stability in PEM fuel cell. Arabian Journal of Chemistry (2019), https://doi.org/10.1016/j.arabjc.2018.12.009

as working electrodes and Pt wire was used as a counter electrode. All experimental potentials were referred to Ag/AgCl, KCl_{sat} as reference electrode. The electrochemical characterization of the modified carbon paste electrodes was carried out by cyclic voltammetry (CV). The CV experiments were recorded in 0.5 M KCl solution containing 1.0 mmol L^{-1} $K_3Fe(CN)_6$ in the potential range of (−0.35) to (+0.8) V at scan rates of 20–120 mV s^{-1}.

The *in-situ* electrochemical measurements were carried out in a single PEMFC system with active area of 25 cm^2 (ElectroChem, USA). A detailed description of the membrane electrode assembly fabrication procedure was reported in our previous studies (Marinoiu et al., 2017, 2017, 2017). To study the effect of adding AuNP/rGO to ORR catalyst, a hybrid cathode was developed. The commercial carbon-supported catalyst (Pt/C catalyst Hispec 4000) was used as both anode and cathode electrodes. A catalyst ink composed of the catalyst mixed with isopropyl alcohol, water and 5 wt% Nafion ionomer solution was sprayed onto the polymer electrolyte membrane (Nafion-212 membrane). The electrodes (anode and cathode) were prepared using an ultrasonic automated spray system (Exacta Coat, Sono-Tek Corporation, USA) by ultrasonic directly spraying. The coating equipment delivers 0.3 mL min^{-1} ink through a 120 kHz ultrasonic nozzle (1.4 W) on substrate heated at 80C. The nozzle followed a serpentine pattern with 1.3 mm brush spacing and a linear speed of 50 mm/sec. The substrate was rotated for a uniform solids deposition.

The Pt loading for anode was established at 0.2 mg_{Pt} cm^{-2} of all developed fuel cells.

The ORR catalyst layer was modified by taking into account two configurations:

(i) Commercial Pt/C catalyst with 0.4 mg_{Pt} cm^{-2} loading, deposited on membrane;
(ii) Pt/C catalyst 0.2 mg_{Pt} cm^{-2} deposited on Nafion membrane and Au/rGO with 0.2 mg_{Au} cm^{-2} loading deposited on carbon paper (gas diffusion layer – GDL Avcarb P75T).

For the MEA made with Pt-based cathode, the state-of-the-art having a loading of 0.2 mg_{Pt} cm^{-2} were used. For the MEA made with AuNP/rGO, the cathode was prepared in-house as described above. It has been demonstrated in our group that a loading of lower than 0.2 mg_{Au} cm^{-2} at the cathode has no considerable effect on the polarization curves and electrochemical stability. MEAs were prepared by hot-pressing at 125 °C for 2 min. using a load of ca. 300 KgF. The cathode was firstly pre-pressed at same temperature for 30 s in order to minimize the risk of altering the membrane during MEA hot pressing. Teflon gaskets were used at both the anode and cathode sides. The gasket thicknesses were chosen to achieve ca. 20% compression of the gas diffusion + catalyst layers. The flow rates for H_2/air were ca. 0.2/1.0 slpm using fully humidified gases.

PEMFC tests in this work were performed using MEAs in a single-cell test fuel cell using an Arbin fuel cell test bench and a Parstat MC Potentiostat with a PMC Booster 10 A and NI-cRIO software. The PEMFC was operated at 0.7 V for 1 h for MEA conditioning. The geometry of the flow channel in bipolar plates was the serpentine type. The humidified gases was fed in counter current -flow into the PEMFC, at 70 °C reaction temperature and pressure (atmospheric and 1 bar applied back pressure, respectively). The cyclic voltammetry measurements were performed in a H_2/N_2 mode cell, from 0.02 to 1.2 V at a scan rate of 0.05 V/s. This condition was expected to accelerate the electrochemical degradation. The flow rates of gases (H_2 and N_2) were adjusted using flow controllers. A polarization curve was then recorded by scanning the cell voltage from open circuit voltage down to 0.3 V at a scan rate of 0.5 mV s^{-1}. In-situ accelerated test stress tests (ASTs) were carried out and analyzed as comparison between Pt/C commercial catalyst and a catalytic system developed for this study, namely Pt/C and prepared AuNP/rGO.

3. Results and discussion

Au nanoparticles supported on graphene oxide nano-sheets have been chemically prepared using a simple procedure via a sequence of preparation steps based on chemical oxidation of graphite, graphene oxide functionalization, exfoliation and reduction, detailed in experimental section. Au nanoparticles were synthesized by the reduction method and adsorbed on graphene-PDDA nanohybrid sheets by electrostatic interaction. Using this strategy, $AuCl_4^-$ ions could be confined in the positively charged surface of PDDA-functionalized graphene and then be in situ reduced to Au nanoparticles upon the addition of reducing agents. A controllable deposition of Au nanoparticles on graphene was performed. The structural characteristics, morphology, composition and electrocatalytic proprieties of prepared samples were evaluated through various characterization techniques.

The morphology of AuNP/rGO samples was characterized by FE-SEM technique. As it can be easily seen, the structure strongly depends on the drying method used. After simultaneous reduction of GO in the presence of PDDA and $HAuCl_4$, the surface of rGO nanosheets was decorated with AuNPs for both samples A and B.

As it can be seen from Fig. 1, AuNPs are distributed all over the surface of functionalized rGO sheets during both proposed synthesis protocol. In the case of lyofilization drying, the graphene layers were stacked together forming bundles with intermixed metal nanoparticles (Fig. 1a, b). Application of conventional drying in oven resulted in the structure of wrinkled features (see Fig. 1c, d).

The surface functional groups of AuNP_rGO samples were investigated by FTIR spectroscopy (Fig. 2). The reduction of GO was depicted base on the weak peaks of ─OH, C═O and O─H bond vibrations situated at 3400, 1720, and 1630 cm^{-1} respectively. In the case of the functionalized and reduced graphene oxide, the intensity of these peaks decreased dramatically or even disappeared.

The functionalization of GO with PDDA is confirmed in spectra of AuNP/rGO nanocomposites for both samples, by appearance of supplementary peaks at 1463 and 850 cm^{-1}, assigned to the N─C bond from characteristic bands of PDDA.

The change of chemical composition during the reduction of GO and functionalization with PDDA and Au nanoparticles was investigated by X-ray photoelectron spectroscopic (XPS). Fig. 3 presents the XPS survey spectra for reduced graphene oxide (rGO) and AuNP/rGO nanocomposites. Main peaks for carbon, oxygen, nitrogen, chlorine and gold are indi-

Please cite this article in press as: Marinoiu, A. et al., Low-cost preparation method of well dispersed gold nanoparticles on reduced graphene oxide and electrocatalytic stability in PEM fuel cell. Arabian Journal of Chemistry (2019), https://doi.org/10.1016/j.arabjc.2018.12.009

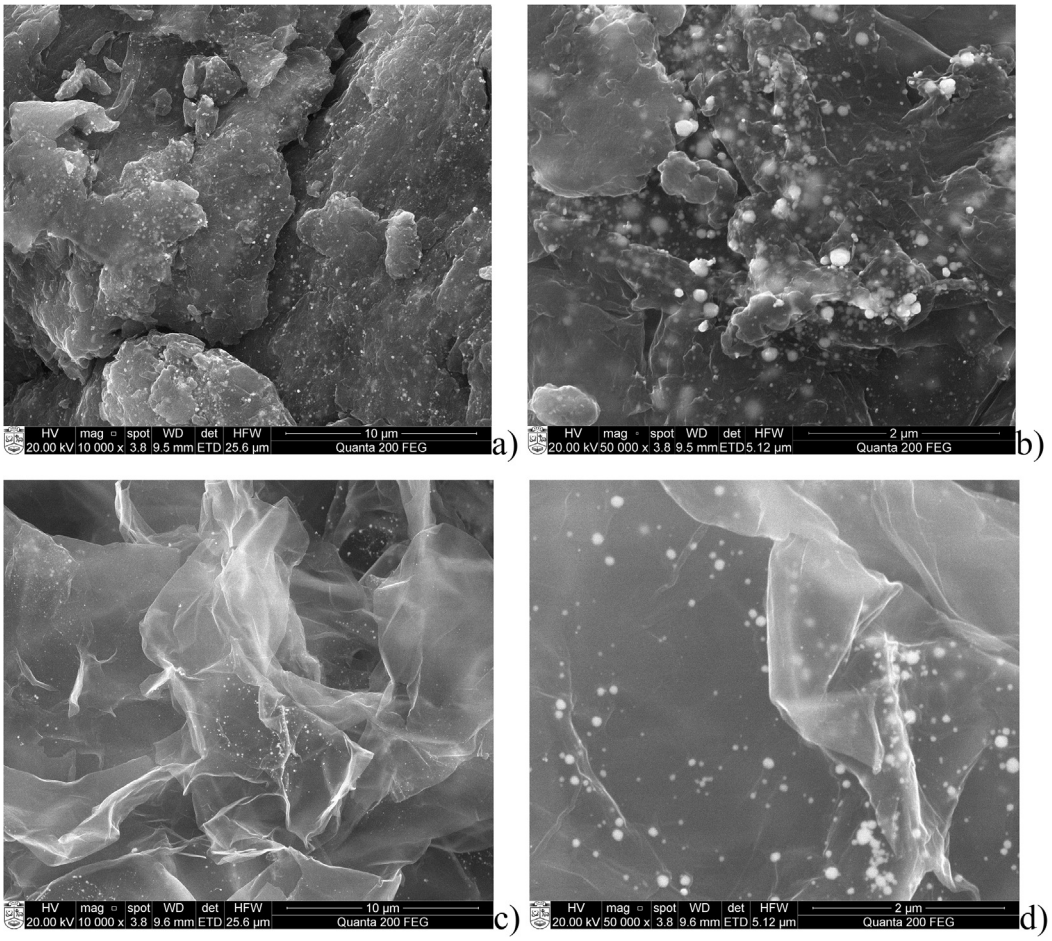

Fig. 1 The SEM images of as-prepared functionalized reduced graphene oxide decorated with gold: AuNP/rGO_A (a and b), AuNP/rGO_B (c and d).

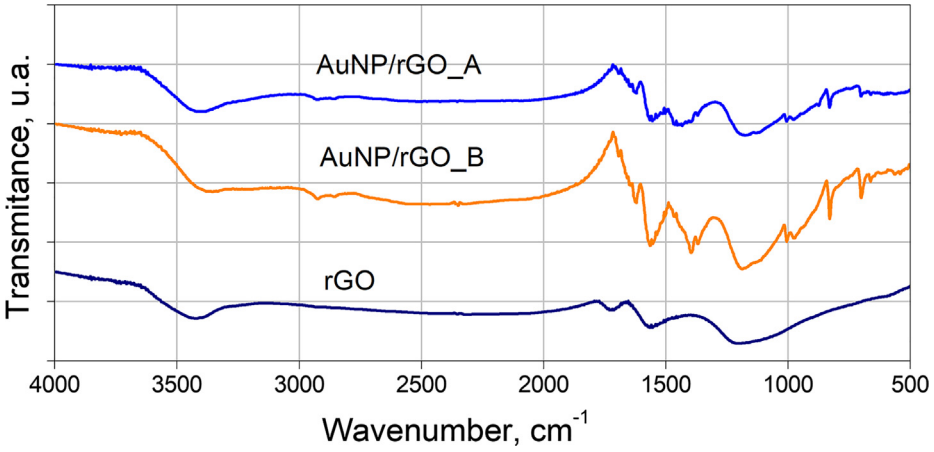

Fig. 2 FT-TIR spectra of graphene oxide and AuNP/rGO nanocomposites.

cated. The appearance of Cl 2p peaks in spectra of AuNP/rGO nanocomposites confirmed the functionalization of rGO with PDDA while Au 4f peak indicated presence of the gold.

High-resolution spectra were scanned (for atomic concentration calculations) and deconvoluted for detailed analysis of possible chemical bonds (Fig. 4a–l). The atomic and weight concentrations of the elements present in the samples are given in the Table 1. AuNP/rGO_A and AuNP/rGO_B samples exhibit similar surface composition. As expected, the O/C atomic ratio decreased as an effect of the $NaBH_4$ reduction, which was accompanied by the appearance of N 1s and Cl 2p peaks. As it is shown in Table 1, the significant amount

Please cite this article in press as: Marinoiu, A. et al., Low-cost preparation method of well dispersed gold nanoparticles on reduced graphene oxide and electrocatalytic stability in PEM fuel cell. Arabian Journal of Chemistry (2019), https://doi.org/10.1016/j.arabjc.2018.12.009

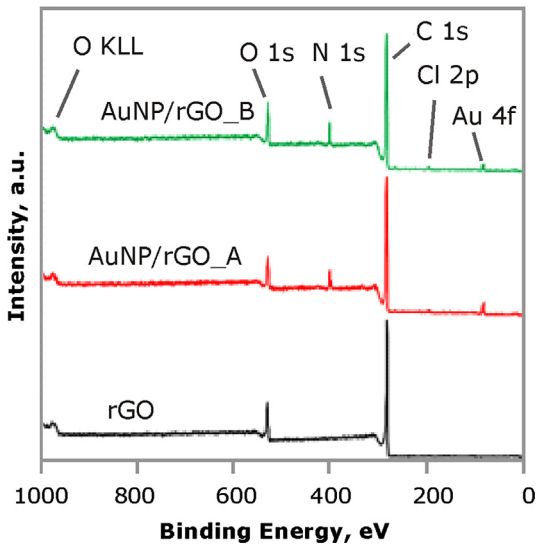

Fig. 3 XPS survey spectra for rGO and AuNP/rGO nanocomposites.

of oxygen was found in the AuNP/rGO nanocomposites (~9 at%) and in rGO sample (~12 at%). The origin of oxygen could be addressed to efficiency of oxidation step. It is also worth to notice that equal amount of nitrogen and chlorine should be expected from the chemical formula of PDDA – $(C_8H_{16}ClN)_n$, nevertheless the N/Cl ratio of 8.43 and 6.23 was obtained for AuNP/rGO_A and AuNP/rGO_B sample, respectively. The reduced amount of chlorine compared to initial PDDA could be explained due to the reaction of Cl^- (from PDDA) with H^+ during reduction process (Kaur et al., 2013). Deconvoluted high-resolution spectra for chlorine in Cl 2p region (Fig. 5g and h) showed Cl $2p_{3/2}$ and Cl $2p_{1/2}$ orbit split doublet located at 197.8 eV and 199.4 eV respectively which could be assigned to chlorine in PDDA (Marinoiu et al., 2017). Low intensity peaks at 201.2 eV and 202.7 eV indicates chlorine bounded to oxygen (NIST, 2003). Both assumptions suggest that applied method B provides less chlorine losses thus preserving unaltered PDDA during rGO functionalization process.

In contrary to chlorine, the amount of nitrogen in AuNP/rGO samples is much larger of that expected from the PDDA formula (theoretical N/C ratio is 1.02). Namely, the C/N ratio calculated from XPS spectra is 5.55% and 5.32% for AuNP/rGO_A and AuNP/rGO_B respectively. These values are similar to reported C/N value of 3.8% for PDDA – carbon nanotubes (CNTs) composite and 13% for pure PDDA in (Wang et al., 2011). Similar effect of nitrogen enrichment was also noticed for PDDA – CNTs composite where the amount of nitrogen increased up to 1.8–14 times (Zhang et al., 2013; Yang et al., 2005) compared to the theoretical composition of PDDA.

Deconvolution of nitrogen high-resolution N 1s spectra for AuNP/rGO nanocomposite samples revealed presence of one main peak and two lower intensity peaks in the spectra. Lowest intensity peak at approximately 404 eV can be assigned to nitrogen-oxygen bonds. The position of main nitrogen N 1s peak at ~403 eV detected for both AuNP/rGO samples (Fig. 7) is typical for pure PDDA (403 eV (Yang et al., 2005) and 403.25 eV) (Kaur et al., 2013), and carbon allotropes functionalized with PDDA (403.25 eV (Kaur et al., 2013) and 403 eV (Yang et al., 2005). Moreover, the lower intensity peak at ~400 eV observed for functionalized samples were also attributed to the PDDA as was previously reported (Dong et al., 2016; Marinoiu, 2017). Appearance of this peak could be due to an uncharged side product (Yang et al., 2005) when PDDA lose part of Cl^+ (Kaur et al., 2013). This assumption coincides with effect of reduced chlorine amount as was discussed in the text above. Calculated ratio of these two peaks (at 403 eV and 400 eV) is 2.2 and 9.6 for the sample AuNP/rGO_A and AuNP/rGO_B samples respectively. These values fit well with other reported results (from 1.8 and 4.6 up to 13.3) (Yang et al., 2005; Dong et al., 2016; Marinoiu, 2017). On another hand, 9.6 value (AuNP/rGO_B sample) indicates that in this sample most of nitrogen is bound to chlorine. This assumption is in agreement with larger amount of chlorine found on the surface of AuNP/rGO_B sample (Table 1). The difference could arise due to loss of chlorine and increased amount of N.

Carbon C 1s spectra for PDDA functionalized rGO was deconvoluted using 7 peaks. These peaks indicate that part of carbon atoms are bound to oxygen or/and hydrogen, though some carbon-nitrogen bonds cannot be excluded also (Fig. 5a and b) considering probable loss of some chlorine from PDDA. The peak at lowest binding energy (284.3 eV) was assigned to C—C bonds (sp^2 configuration) – the binding energy value is close or identical to reported in (Marinoiu et al., 2017, 2016; Bertoti et al., 2015; Bayev et al., 2018; Vinayan et al., 2016) for C—C sp^2 bonds. This peak was fitted using 20:80 Gauss-Lorentz function and asymmetrical shape due to conductive nature of sp^2 carbon (Kahlert et al., 2014.). Peak at ~284.9 eV was assigned to C—C bonds (sp^3 configuration) – similar value of binding energy is reported in (Bertoti et al., 2015; Bayev et al., 2018; Marinoiu et al., 2016; Vinayan et al., 2016). It should be noted that binding energy values of 284.8 eV and 285.2 eV for C—C and C—H bonds respectively was reported in (Bertoti et al., 2015) for graphene oxide and pristine graphene respectively, therefore this peak most likely represents both C—C (sp^3) and C—H bonds. Calculation of sp^3/sp^2 ratio showed similar values (4.6 and 3.67 for NP/rGO_A and AuNP/rGO_B respectively) for both samples. The difference could arise due to chlorine losses and increase of N^0 content – this effect could provide possibility for part of graphene to restack into graphite form (Wang et al., 2011) as was noticed in composite preparation part.

The rest of fitted C 1s spectra for PDDA functionalized rGO samples consist of the most intense peak (~30%) at 285.7 eV, two lower intensity peaks at approximately 286.5 eV and 287.2 eV and two low intensity (less than 6%) peaks at 288.1 eV and 289.5 eV. The most intense peak at 285.7 eV was assigned to C—O—C bonds – similar binding energy value (285.5 eV) was found on surface of the C_3N film (Lazauskas et al., 2016) for these bonds. In addition, almost the same binding energy value was reported for C—N sp^2 bonds (285.8 eV) in N doped graphene (Lin et al., 2010) while in our case C-N bonds could originate from PDDA due to partial chlorine loss. Therefore, it is adequate to state that both components contribute to this peak, and C—O—C bonds could be dominant contributor since the ratio of O/N atomic concentrations is about 2.0 for both AuNP/rGO_A and AuNP/rGO_B samples. Fitted peaks at approximately 286.5 eV,

Please cite this article in press as: Marinoiu, A. et al., Low-cost preparation method of well dispersed gold nanoparticles on reduced graphene oxide and electrocatalytic stability in PEM fuel cell. Arabian Journal of Chemistry (2019), https://doi.org/10.1016/j.arabjc.2018.12.009

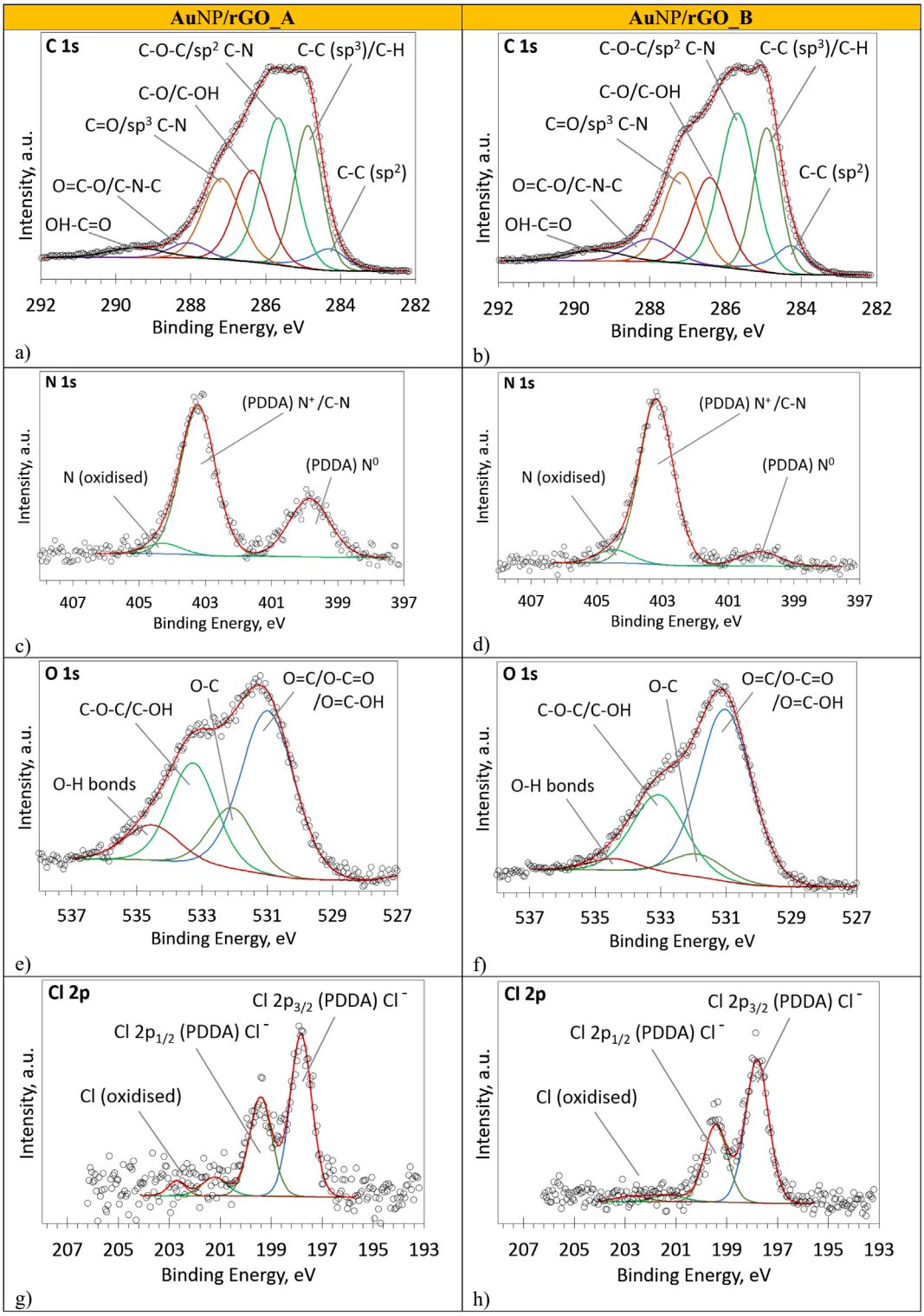

Fig. 4 The high-resolution XPS spectra of AuNP/rGO nanocomposites and rGO.

287.2 eV, 288.1 eV and 289.5 eV were assigned to C—O/C—OH, C═O/C—N sp^3, O═C—O/C—N—C and O═C—OH bonds respectively. Similar binding energy values were reported for these bounds: C—O/C—OH (286.3 eV and 286.4 eV) (Marinoiu et al., 2017); C═O (287.3 eV and 287.7 eV) (Borowiec et al., 2015; Bertoti et al., 2015) and C—N sp^3 (287.1 eV) (Bertoti et al., 2015); O═C—O (288.3 eV) (Bayev et al., 2018) and C—N—C (282.0 eV) (Lazauskas et al., 2016); O═C—OH (289.3 eV and 289.6 eV) (Borowiec et al., 2015; Bertoti et al., 2015). These peaks indi-

Please cite this article in press as: Marinoiu, A. et al., Low-cost preparation method of well dispersed gold nanoparticles on reduced graphene oxide and electrocatalytic stability in PEM fuel cell. Arabian Journal of Chemistry (2019), https://doi.org/10.1016/j.arabjc.2018.12.009

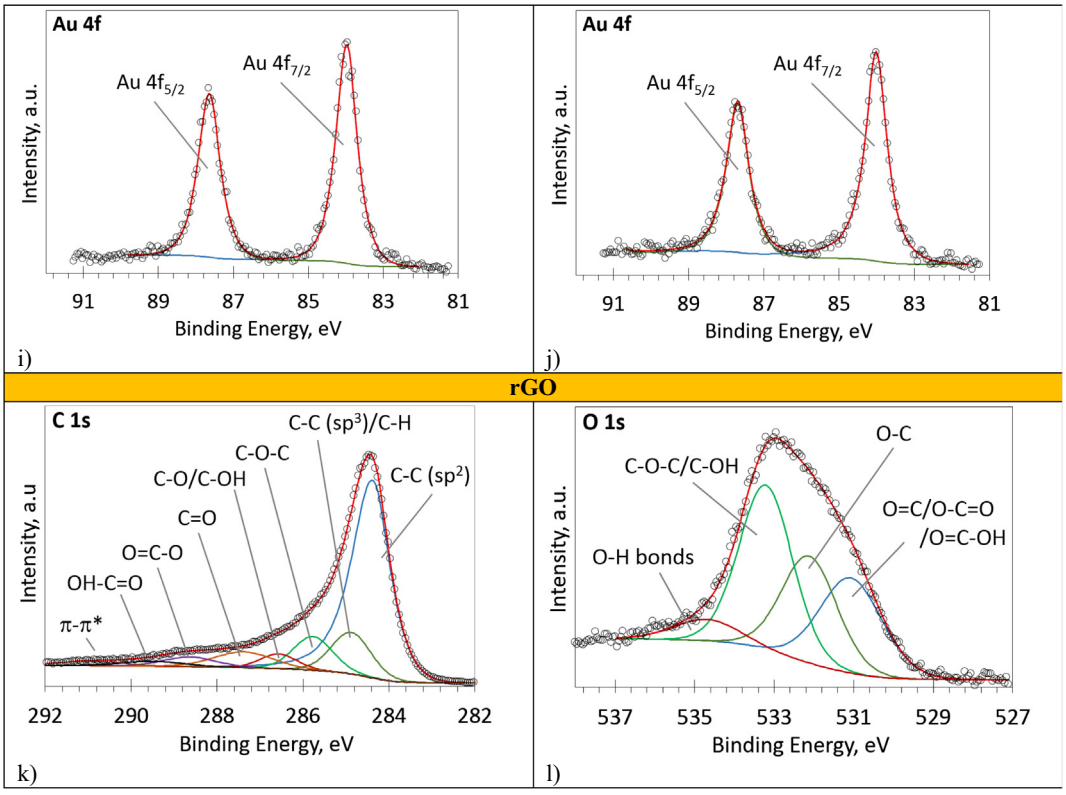

Fig. 4 (*continued*)

Table 1 Chemical compositions for AuNP/rGO nanocomposites.

Element	Atomic concentrations, %			Weight concentrations, %		
	AuNP/rGO_A	AuNP/rGO_B	rGO	AuNP/rGO_A	AuNP/rGO_B	rGO
O 1s	9.12	9.19	12.43	11.09	11.34	12.89
N 1s	4.72	4.55	–	5.03	4.91	–
C 1s	85.3	85.35	87.57	77.88	79.02	87.11
Cl 2p	0.56	0.73	–	1.51	1.99	–
Au 4f	0.3	0.18	–	4.49	2.73	–
C/O ratio	9.35	9.29	7.1	7.02	6.96	6.75

cate considerable amount of carbon – oxygen bonds most likely due to atmospheric contaminants or/and PDDA surface oxidation or some residuals of graphene oxide.

In deconvoluted high-resolution C 1s spectra of rGO sample (Fig. 5k) one can see that the fitted peak at 284.4 eV dominates (60%). The asymmetrical shape of this peak is typical for C—C sp^2 bonds in graphene (Kahlert et al., 77, 2014.). The low intensity peak at 290.9 eV could be assigned to π-π shake up satellite (Bertoti et al., 2015). The majority of carbon-oxygen bonds most likely represents adsorbed atmospheric contaminants or/and some residuals of graphene oxide, while low sp^3/sp^2 ratio value (0.2) indicates high efficiency of applied reduction process.

Oxygen spectra in O 1s region was deconvoluted using 4 curves for AuNP/rGO_A, AuNP/rGO_B and rGO samples as shown in Fig. 5e, f, l respectively. The lowest intensity peak at ~534.5 eV was observed in the spectra of all samples and was attributed to O—H bonds in water (NIST, 2003). As the intensity of this peak is smallest for the sample AuNP/rGO_B, it could be stated that it adsorbed less moisture compared to the other samples. The peak at 531 V was attributed to O═C/O—C═O/O═C—OH bonds – position of this peak coincides with reported positions for O = C (530.6 eV, 531.0 eV and 531.4 eV) (Bertoti et al., 2015; Marinoiu et al., 2016; Vinayan et al., 2016) O—C═O (530.6 eV and 531.2 eV) (Bertoti et al., 2015; Jankauskaite et al., 2016), O═C—OH (530.8 eV) (Song et al., 2016) bonds. This peak is dominant in O 1s spectra for AuNP/rGO samples and is lower intensity for rGO sample. In contrary, peak at 533.2 eV is dominant for rGO sample and is less pronounced for AuNP/rGO samples. This peak was attributed to C—O—C and C—OH bonds (Bertoti et al., 2015; Wang et al., July 2014). Third peak at 532.1 eV was assigned to C—O bonds (Jankauskaite et al., 2016). Noticeable, intensity of C—O—C/C—OH and C—O peaks for sample AuNP/rGO_B correlates with lower intensity of O-H peak when compared with these peaks for AuNP/

Please cite this article in press as: Marinoiu, A. et al., Low-cost preparation method of well dispersed gold nanoparticles on reduced graphene oxide and electrocatalytic stability in PEM fuel cell. Arabian Journal of Chemistry (2019), https://doi.org/10.1016/j.arabjc.2018.12.009

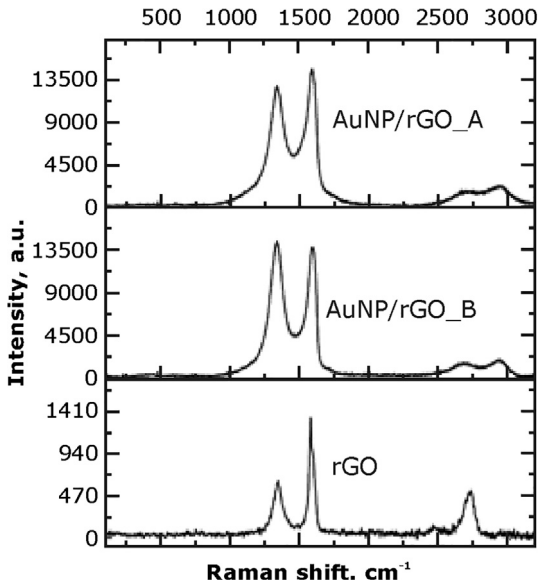

Fig. 5 Raman spectra for rGO and AuNP/rGO samples.

rGO_A sample. The difference of intensity of these three peaks in rGO and AuNP/rGO most likely arise due to different surface adsorption properties of the samples thus providing different amount of adsorbed atmospheric contaminants.

Only two peaks were detected in Au 4f spectra (Fig. 5i and j) of AuNP/rGO samples. Deconvolution of Au 4f region showed two asymmetrical peaks best fitted using 80:20 Lorenz-Gauss function. Position of these peaks at 84.0 eV and 87.7 eV are in good agreement with known orbit-split doublet positions of Au $4f_{7/5}$ and Au $4f_{5/2}$ peaks (Wang et al., 2011) for Au^0. Position and shape of these peaks confirms the presence of metallic gold on the surface of functionalized rGO samples and suggests its successful decoration with gold nanoparticles. As shown in Au 4f spectrum of AuNP/rGO, only doublets of Au 4f5/2 and Au 4f7/2 were observed, indicating absence of Au^{2+} and Au^{4+} oxidation states. It is worth noting that gold nanoparticles existed only in metallic form despite the existence of a large amount of oxygen-containing functional groups in PDDA-functionalized rGO.

The Raman spectra of rGO and AuNP/rGO samples were analyzed. The Raman spectra provided in Fig. 6 indicate the presence of all characteristic bands of few layer graphene with structural defects. The AuNP/rGO composites have similar characteristic Raman peaks, which corresponds to the D and G bands from GO sheets. Three strong bands appeared at 1344–1347 cm^{-1} (D band – associated with the presence of structural defects), 1588–1591 cm^{-1} (G band – characteristic of all sp^2 – based materials), and a D-peak overtone band at about 2675–2680 cm^{-1} (2D). Additionally, to these bands, in the case of nanocomposite samples, the D + G combination band was observed around ~2919 cm^{-1} that is induced by disorder in the structure (Antony et al., 2015). The position and intensity of the peaks was determined by approximation using Lorentzian profile and summarized in Table 2.

The 2D band intensity is generally very sensitive to the number of layers in the graphene structure. The relative intensity ratio of the D and G bands (I_G/I_D) may be associated with the number of defects within the graphene sheets and the in plane sp^2 crystallite size L_a (Hafiz et al., 2014). Generally, the I_D/I_G ratio increases when more defects are brought into GO. Due to further functionalization of rGO, the D band intensity increased dramatically and I_D/I_G ratios (Table 2) corresponding to AuNP/rGO composites were much higher (1.02 and 0.85 for sample A and B respectively) compared with rGO (0.51). The results illustrate that the loading amount of Au NPs has strong influence on the ratio, implying that the nucleation of gold nanoparticles at rGO surfaces introduces additional defects into structure.

Heteroatom-doped graphenes are well known for its largely exposed surface that interacts, therefore, evaluating the surface area is a crucial step in understanding and optimizing their performance. Currently, the most reliable method to evaluate the surface area is the classical BET method, which derives from nitrogen sorption isotherms collected at 77 K (Comparison of Average Number of Stacked Layers).

However, graphene sheets tend to stack on top of each other due to weak but extensive van der Waals interactions between their surfaces, which may appear quite likely during the chemical synthesis. Fig. 6 shows the nitrogen adsorption-desorption isotherms and the corresponding pore size distribution curves of rGO and AuNP/rGO composites. Lower pressure region (quite similar to Type II) and intermediate flat region in the isotherms correspond to the formation of monolayer. At higher pressures the slope presents increased uptake of adsorbate as pores become filled, inflection point typically occurs near completion of the first monolayer followed by multilayer. The curves of studied samples are type IV (according to IUPAC classification), describing the adsorption behavior of porous adsorbents and indicating the presence of mesopores mainly, micropores and some macropores, together with hysteresis behavior between the adsorption and the desorption branch. A hysteresis appeared, with the shape of loops in-between type H3, assigned to the process of capillary condensation of nitrogen, and type H4, relative to the presence of pores with the shape of thin slots formed between two surfaces, indicating that the cleft-like pores were formed by the aggregation of platelets-like particles. The pores in an efficient ORR catalyst layer must act two complementary roles, namely the primary pores work as reaction volume, while secondary pores play the gas channel role in the porous structure.

Pore size distribution data was obtained from desorption branches of isotherms using Barrett-Joyner-Halenda (BJH) method and are illustrated as insets in Fig. 6. The results of surface area, pore volume, and pore radius are listed in Table 3. The BET specific surface area decreased from 245 $m^2\,g^{-1}$ for rGO to 87 and 52 $m^2\,g^{-1}$ for AuNP/rGO_A and AuNP/rGO_B, respectively and may be attributed to reduced porosity due to functionalization with Au nanoparticles. The measured surface area of functionalized graphene samples is consistent with the stacking structure and agglomerated morphology of the reduced graphene sheets.

BJH pore radius of 1.967 nm corresponding to rGO was close to the pore radius of gold doped graphene AuNP/rGO_A and AuNP/rGO_B (1.567 nm and 1.875 nm respectively), while cumulative pore volume (2.214 $cm^3\,g^{-1}$) is much bigger than doped graphene (0.112 $cm^3\,g^{-1}$ and 0.083 $cm^3\,g^{-1}$), indicating that a large number of mesopores have been clogged during doping process. The mentioned radii implied a hierarchical interconnected porous framework in doped graphene structure. It is known that different pore type displayed differ-

Please cite this article in press as: Marinoiu, A. et al., Low-cost preparation method of well dispersed gold nanoparticles on reduced graphene oxide and electrocatalytic stability in PEM fuel cell. Arabian Journal of Chemistry (2019), https://doi.org/10.1016/j.arabjc.2018.12.009

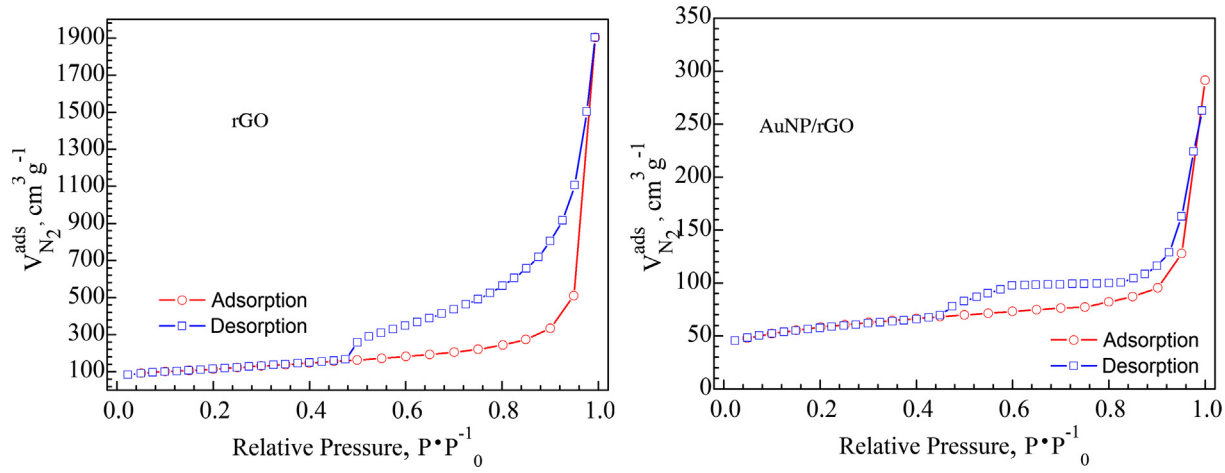

Fig. 6 Nitrogen adsorption-desorption isotherms and the corresponding pore size distribution for undoped rGO and AuNP/rGO.

Table 2 Raman characteristics for AuNP/rGO composites.

Sample	Intensity (counts)				Band positions (cm^{-1})				
	D band	G band	D' band	D/G intensity ratio	D band	G band	D' band	2D band	D + G band
AuNP/rGO_A	13915.9	13561.1	–	1.03	1344	1591	–	2675	2919
AuNP/rGO_B	11784.3	13759.1	–	0.86	1347	1588	–	2680	2920
rGO	567	1092.1	525.7	0.52	1351	1582	1605	2709	–

Table 3 Textural proprieties of rGO and gold-doped graphene.

Samples	S_{BET} ($m^2\ g^{-1}$)[a]	BJH Pore volume[b] ($cm^3\ g^{-1}$)	BJH Pore Radius (nm)
AuNP/rGO_A	87	0.112	1.567
AuNP/rGO_B	52	0.083	1.875
rGO	245	2.214	1.967

[a] BET surface area calculated from the linear part of the BET plot (P/P_0 = 0.1–0.3).
[b] Pore volume, taken from the volume of N_2 adsorbed at P/P_0 = 0.99, using BJH method.

ent roles in the PEMFC electrochemical performance (Avcioglu et al., 2015; Marinoiu et al., 2015). Their existence could offer sufficient space to allow access of the reactants to the catalytic sites and would accelerate the kinetic process of ion diffusion. Thus, such hierarchical porous nanomaterials, which facilitated solid electrolyte membrane penetration and ion diffusion, could be ideal for the high-performance electrode for PEMFC.

To evaluate the redox behavior of the AuNP/rGO samples, the cyclic voltammetry measurements using carbon paste modified electrodes (as described in experimental section) were performed. The electrochemical characterization of the electrodes modified with AuNP/rGO was undertaken in order to evaluate their electrochemical efficiency by using the ferro/ferricyanide redox probe (Marinoiu et al.) and the electroactive areas, respectively. For this purpose, parallel experiments with electrodes made of bare carbon paste and modified graphene oxide electrodes were performed. In addition, for a better evaluation of these modified electrodes, similar experiments with glassy carbon as working electrodes were performed. In all cases, the experimental results showed well defined and reproducible anodic and cathodic peaks related to $Fe(CN)_6^{3-}/Fe(CN)_6^{4-}$ redox couple with a quasi reversible behavior. The peak separation potential ΔEp (Epa − Epc) was observed between 180 and 325 mV for all electrodes. A comparison of electrodes CV measurements is presented in Fig. 7.

Analysis of the cyclic voltammograms revealed that all modified electrodes exhibit an enhancement of the current response when compared to classical glassy carbon which translates in better electrocatalytic activity for both oxidation and reduction processes. Moreover, comparing the performance of rGO modified electrode with the AuNP/rGO the positive effect of the metal was obvious. The best results were obtained for AuNP/rGO_A modified electrode for which the current was 3.94 times higher comparing with the CPE. Also, the anodic and cathodic peak potentials are shifted by around −100 mV for AuNP/rGO_A and −80 mV for AuNP/rGO_B, comparing with the potential of CPE. Electrochemical data and areas of the used electrodes are presented in Table 4.

An increase in the peak currents and a decrease in the separation between the peak potentials (ΔEp) of 20 mV s^{-1} were observed for all modified electrodes in comparison to the bare carbon paste electrode, indicating that the electron transfer reaction was kinetically and thermodynamically favored at the used electrode surface (see Table 4). The electroactive areas of carbon-paste modified electrodes was calculated according

Please cite this article in press as: Marinoiu, A. et al., Low-cost preparation method of well dispersed gold nanoparticles on reduced graphene oxide and electrocatalytic stability in PEM fuel cell. Arabian Journal of Chemistry (2019), https://doi.org/10.1016/j.arabjc.2018.12.009

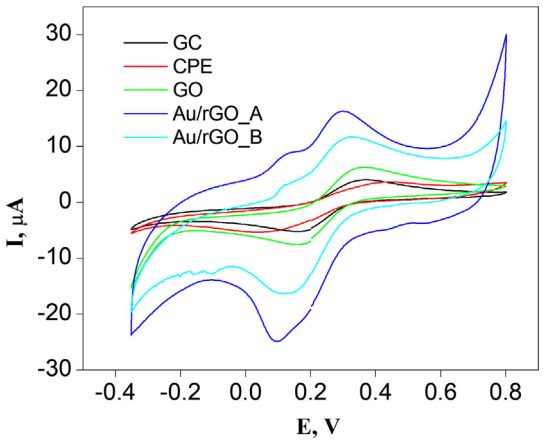

Fig. 7 Cyclic voltammograms for 1.0 mM $K_3Fe(CN)_6$ in 0.5 M KCl solution at v = 20 mV s^{-1}.

to Randles–Sevcik equation using the slope of the I_a *versus* square root of the scan rates plot for the studied redox probe, namely 1.0 mM $K_3[Fe(CN)_6]$ solution in 0.50 M KCl electrolyte:

$$I_a = 2.69 \cdot 10^5 \cdot n^{3/2} \cdot D^{1/2} \cdot A \cdot c \cdot v^{1/2}$$

where I_a is the anodic peak current, n – number of transferred electrons, A –electroactive area of the electrode, D is the diffusion coefficient, v is the scan rate and c is the concentration of potassium ferrocyanide solution.

The microscopic areas presented in Table 4 were calculated for n = 1 and D = 6.68×10^{-6} cm^2 s^{-1} using the slope of the Ip–$v^{1/2}$ relation. Analysis of the data revealed the positive effect of the gold component in the modified electrodes. Comparing the non-metallic modified graphene oxide (GO) electrode (entry 3, Table 4) with both AuNP/rGO electrodes, the superior performance of the latter was observed. The determined values of electroactive surface (entries 4 and 5) suggest that these materials could be used as electrocatalysts for ORR reaction in fuel cells. However, comparison between the two AuNP/rGO electrodes (A (entry 4) and B (entry 5)) show that the preparation of the composite is crucial for the resulting electrochemical efficiency.

The effect of varying the voltammetric scan rate is very useful because by increasing the scan rate, the current of the adsorption peak increases in magnitude. Therefore the AuNP/rGO electrodes were tested for $Fe(CN)_6^{3-}/Fe(CN)_6^{4-}$ redox couple at scan rate from 20 to 120 mV/s (Figs. 8 and 9). As the scan rate was increased, the current for both anodic and cathodic peak also increased and both peak potentials remained almost unchanged over the chosen scan rate range. These cyclic voltammograms were used to monitor the variation of the voltammetric response as a function of scan rate (*v*). The plot of the peak height *versus* square-root of the scan rate is illustrated in Fig. 8(b) and Fig. 9(b). The shape of the voltammograms and their variation with the scanning speed is similar for both samples, also the variation of the potential (oxidation and reduction) has a linear dependence on speed. Both, the anodic and the cathodic peak currents reveal linear response at all scan rates with very good correlation factors, R^2 = 0.992 for the oxidation peak and R^2 = 0.999 for the reduction peak. This is indicative of a diffusion-controlled electrochemical process.

In conclusion, the electrochemical performance for ferri/-ferro redox process is higher for Au/rGO_A modified electrode, its sensitivity at higher scanning rates showing well defined peaks. Thus, benefiting from unique features, the developed Au/rGO_A material indicated good electrochemical performances as possible electrodes. The challenge of achieving an electrochemical stability is considered especially difficult because, for ORR catalysts, the role of support should be combined with the role of catalyst. So, while the microporosity is required to obtain high catalytic activity and a high mesoporosity is required for an efficient transport of ORR related species (O_2, H_2O and protons) in the catalyst layer, moreover, a nanostructured catalyst with high stability in acid media is necessary. In this work, we explored the use of AuNP/rGO as co-catalyst in creating of an improved ORR cathode which includes: Pt/C catalyst that assures the ORR catalytic activity, and AuNP/rGO that allows a high electrochemical stability of cathode catalytic system.

Electrical performance of developed cathode was performed by polarization curve (Fig. 10). In order to evaluate the power density, a fuel cell voltage of 0.6 V is recommended, because it provides an accurate balance between energy efficiency and power density for well performing electrocatalysts. The membrane electrode assembly (MEA) using the developed cathode and tested in PEM fuel cell, produced a peak power density of 0.65 W cm^{-2} and a power density of 0.59 W cm^{-2} at 0.6 V, the latter comparable with that of a state-of-the-art platinum-based cathode having a loading of 0.3 mg_{Pt} cm^{-2} (Peng et al., 1765; Proietti et al., 2011).

In order to validate the previously *ex-situ* CV results, AuNP/rGO material was involved in fabrication of a hybrid cathode, as follows: commercial Pt/C 0.2 mg_{Pt} cm^{-2} loading was deposited on Nafion membrane and prepared AuNP/rGO with 0.2 mg_{Au} cm^{-2} loading was deposited on carbon paper. These two layers form a novel ORR catalytic system

Table 4 Electrochemical data from CV measurements at 20 mV/s.

Entry	Electrode type	I_a (μA)	I_c (μA)	ΔE (mV)	A (cm^2)
1.	GC	3.79	−4.10	181	0.0706
2.	CPE*	2.40	−3.23	325	0.0165
3.	GO*	6.14	−5.99	182	0.0309
4.	AuNP/rGO_A	9.45	−1.47	200	0.2020
5.	AuNP/rGO_B	7.93	−9.45	241	0.0999

* Notes: I_a and I_c represent the anodic and cathodic peak currents, ΔE is the separation between the peak potentials and A is the area of an electrode, with the corresponding measurements units described in reference (Marinoiu et al.).

Please cite this article in press as: Marinoiu, A. et al., Low-cost preparation method of well dispersed gold nanoparticles on reduced graphene oxide and electrocatalytic stability in PEM fuel cell. Arabian Journal of Chemistry (2019), https://doi.org/10.1016/j.arabjc.2018.12.009

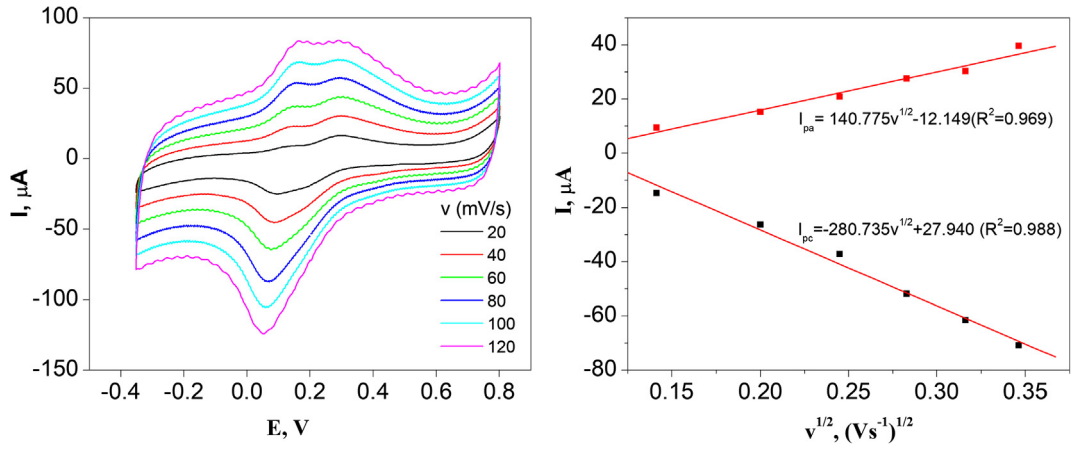

Fig. 8 Cyclic voltammograms for 1.0 mM $K_3Fe(CN)_6$ in 0.5 M KCl solution for AuNP/rGO_A electrode, v = 20–120 mV s^{-1} (a) plot I vs. $v^{1/2}$ (b).

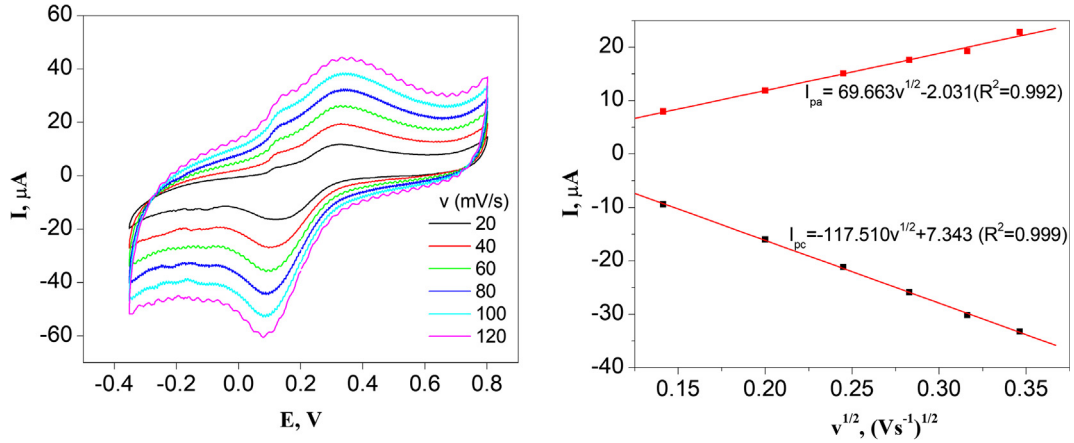

Fig. 9 Cyclic voltammograms for 1.0 mM $K_3Fe(CN)_6$ in 0.5 M KCl solution for AuNP/rGO_B electrode, v = 20–120 mV s^{-1} (a) plot I vs. $v^{1/2}$ (b).

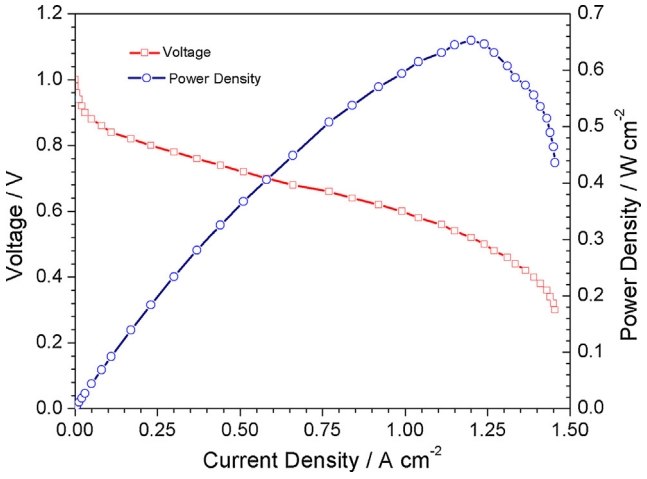

Fig. 10 Polarization curve plot and Power density plot of a hydrogen-air PEMFC including developed cathode (with AuNP/rGO); Cell runs with H_2/air at 1 bar anode and cathode back pressure and 70 °C fuel cell temperature.

which was evaluated in comparison to cathode containing no Au/rGO. In actual study, the Pt loading was established at 0.2 mg_{Pt} cm^{-2} for anode of both developed fuel cells. The cathode catalyst layer was evaluated in two configurations: (i) commercial Pt/C catalyst with 0.4 mg_{Pt} cm^{-2} loading (test 1); developed ORR catalytic system, including commercial Pt/C 0.2 mg_{Pt} cm^{-2} and prepared Au/rGO Pt/rGO with 0.2 mg_{Pt} - cm^{-2} loading (test 2).

Taking into account the application of Au/rGO_A material as ORR electrode for PEMFC, the *in-situ* electrochemical accelerated stress tests (ASTs) at potentials above 0.0 V_{SHE} were carried out in order to accelerate the degradation of catalysts aiming to assess their durability. The state of the art data highlights that the potential cycling may cause the remarkable most relevant changes of the catalyst structure. Overall, the carbon corrosion at cathode side must be understood as a structural breakdown of support from ORR catalyst, which results in the separation or/and agglomeration of Pt particles. Thus, the catalyst involvement in accelerated test was focused on potential cycling between 0.0 and 1.2 V_{SHE}, which theoretically cause a fast catalyst aging, in contrast to a constant potential keeping test.

Please cite this article in press as: Marinoiu, A. et al., Low-cost preparation method of well dispersed gold nanoparticles on reduced graphene oxide and electrocatalytic stability in PEM fuel cell. Arabian Journal of Chemistry (2019), https://doi.org/10.1016/j.arabjc.2018.12.009

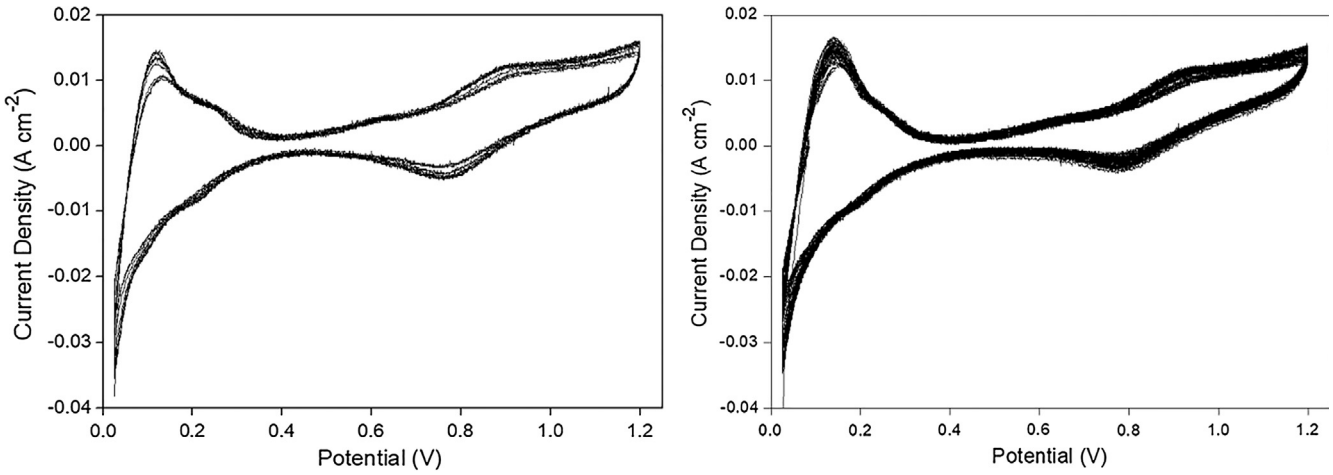

Fig. 11 Cyclic voltammetry of commercial Pt/C for 50 cycles in following operation conditions: temperature 70 °C; scan rate 50 mV/s; atmospheric pressure (a) and 1 bar (b).

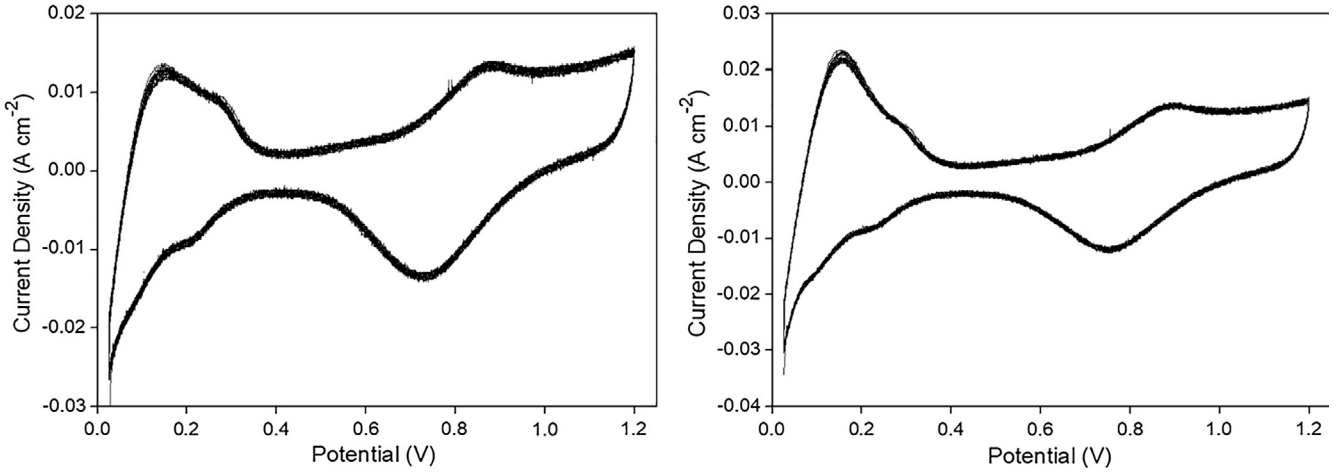

Fig. 12 Cyclic voltammetry of developed ORR catalytic system for 50 cycles in following operation conditions: temperature 70 °C; scan rate 50 mV/s; atmospheric pressure (a) and 1 bar (b).

Figs. 11 and 12 present the cyclic voltammogrames corresponding to catalysts exposure to 50 cycles between 0.02 and 1.2 V potential cycling for 2 cases: (i) commercial Pt/C and (ii) developed catalytic system Pt/C – AuNP/rGO respectively. During the forward voltage sweep in the corresponding CV measurement (0.05–0.4 V), the protons permeates through the membrane, then are adsorbed on the metal surface from the cathode side. In the backward voltage sweep the generated H^+ is then adsorbed and oxidized on the Pt surface. The hydrogen desorption peak at around 0.2 V during the forward scan decreased during AST mainly in FC operation condition corresponding to 1 bar pressure. Moreover, the CV results showed that the oxidation and reduction peaks corresponding to hydrogen adsorption/desorption (0.025–0.3 V) decreased differently during AST, indicating that a decrease of electrochemical surface area occurs for both cases, more visible for commercial catalyst.

Some observations appear, namely:

- the shapes of curves are fairly similar for the two samples demonstrating that they generate well-defined adsorption/desorption hydrogen regions. Although, it seems numerically easy to evaluate the electrochemical surface area, the validity of this area approach is questionable as it assumes that the contributions from the platinum and gold are independent;
- the MEA including AuNP/rGO as ORR catalyst showed a good electro-stability in PEMFC durability tests.

Moreover, it is easily to notice the change in hydrogen adsorption/desorption on commercial Pt single catalyst both for hydrogen oxidation and hydrogen reduction (Fig. 10). The lower PEMFC performance in the first case was attributed to the mass transport limitations and carbon corrosion caused by carbon support.

As regards the developed hybrid catalyst, insignificant changes were noticed for reduction signal, suggesting the

Please cite this article in press as: Marinoiu, A. et al., Low-cost preparation method of well dispersed gold nanoparticles on reduced graphene oxide and electrocatalytic stability in PEM fuel cell. Arabian Journal of Chemistry (2019), https://doi.org/10.1016/j.arabjc.2018.12.009

potential of using Au/rGO as ORR catalyst for future AST durability investigation. Such behavior may be assigned to:

(i) long-term stability and superior conductivity of Au based catalyst fulfilling in this case the role of co-catalyst;
(ii) hydrophilic nature of graphene oxide support, which comports like a water reservoir leading to a better hydration of membrane. Thus a lower ohmic resistance and higher proton conductivity are expected. The detailed long-term durability tests of PEMFC with Au/rGO catalyst and the degradation studies in different PEMFC conditions are ongoing studies.

4. Conclusions

In this research, graphene oxide nanosheets were functionalized with cationic PDDA and decorated with gold nanoparticles. Au nanoparticles were synthesized by the reduction method and then adsorbed on graphene-PDDA nanohybrid sheets by electrostatic interaction. The electrochemical measurements revealed an enhanced performance of the electrode after addition of AuNP/rGO modified electrode. Sharp and well-resolved peaks are observed when CV experiments were utilized. The anodic and cathodic peaks are higher for graphene oxide modified carbon paste electrodes with the higher peak current observed for gold doped reduced graphene oxide. After CV durability testing, the performance loss between the Pt/C and developed electrode based on Pt/C – Au/rGO were observed to be smaller for hybrid electrode. In summary, a novel AuNP/rGO catalyst with a graphene structure was successfully prepared by a low-cost synthesis. The addition of this material to Pt-based catalyst exhibited a high electrocatalytic stability for the ORR in an acidic medium. The Au–graphene electrocatalytic system can be potentially further developed for possible applications as cathodic ORR electrode in PEMFC.

Acknowledgements

This work is supported by the National Agency of Scientific Research from Romania by the National Plan of R & D, Project PN 18 12 01 02. The first author wish to thank Prof. Sigitas Tamulevičius –Director of Institute of Materials Science, Kaunas University of Technology, Lithuania, for his precious help and facilitating access to institute infrastructure during Inter-academic exchange Romania-Lithuania 2017, on the theme "Unconventional electrodes investigation for PEM fuel cells based on graphene materials".

References

Antony, P., Preethi, L.K., Gupta, Bhavana, Tom Mathews, S., Dash, A.K. Tyagi, 2015. Efficient electrocatalytic performance of thermally exfoliated reduced graphene oxide-Pt hybrid. Mater. Res. Bull. 70, 60–67.

Avcioglu, G.S., Ficicilar, B., Bayrakceken, A., 2015. Eroglu I. High performance PEM fuel cell catalyst layers with hydrophobic channels. Int. J. Hydrogen Energy 40, 7720e31.

Bayev, V.G., Fedotov, J.A., Kasiuk, J.V., Vorobyova, S.A., Sohor, A. A., Komissarov, I.V., Kovalchuk, N.G., Prischepa, S.L., Kargin, N.I., Andrulevičius, M., Przewoznik, J., Kapusta, C.Z., Ivashkevich, Tyutyunnikov, S.I., Kolobylina, N.N., Guryeva, P.V., 2018. CVD graphene sheets electrochemically decorated with "core-shell" Co/CoO nanoparticles. Appl. Surf. Sci. 440 (15), 1252–1260.

Bertoti, Imre, Mohai, Miklos, Laszlo, Krisztina, 2015. Surface modification of graphene and graphite by nitrogen plasma: determination of chemical state alterations and assignments by quantitative X-ray photoelectron spectroscopy. Carbon 84 (1), 185–196.

Borowiec, Joanna, Yan, Kai, Tin, Chin-Che, Zhang, Jingdong, 2015. Synthesis of PDDA functionalized reduced graphene oxide decorated with gold nanoparticles and its electrochemical response toward levofloxacin. J. Electrochem. Soc. 162 (3), 164–169.

Cheng, K., He, D., Peng, T., Lv, H., Pan, M., Mu, S., 2014. Porous graphene supported Pt catalysts for proton exchange membrane fuel cells. Electrochim. Acta 132, 356–363.

Comparison of Average Number of Stacked Layers (N) of Commercial Graphene Samples Estimated by Gas Sorption with Reported Values https://www.quantachrome.com/general_pdf/graphene.pdf.

Dong, Lili, Zhang, Xiuqiang, Ren, Suxia, Lei, Tingzhou, Sun, Xiuxuan, Qic, Yadong, Wu, Qinglin, 2016. Poly(diallyldimethylammonium chloride)–cellulose nanocrystals supported Au nanoparticles for nonenzymatic glucose sensing. RSC Adv. 6, 6436.

Gasteiger, H.A., Kocha, S.S., Sompalli, B., Wagner, F.T., 2005. Activity benchmarks and requirements for Pt, Pt alloy, and non-Pt oxygen reduction catalysts for PEMFCs. Appl. Catal. B 56, 9–35.

Hafiz, Syed Muhammad, Ritikos, Richard, Whitcher, Thomas James, Nadia, Md, Razib, Daniel Chi, Bien, Sheng, Chanlek, Narong, Nakajima, Hideki, Saisopa, Thanit, Songsiriritthigul, Prayoon, Huang, Nay Ming, Rahman, Saadah Abdul, 2014. A practical carbon dioxide gas sensor using room-temperature hydrogen plasma reduced graphene oxide. Sens. Actuators B 193, 692–700.

Hellman, H.L., Van den Hoed, R., 2007. Characterizing fuel cell technology: challenges of the commercialization process. Int. J. Hydrogen Energy 32, 305–315.

Hsieh, S.H., Hsu, M.C., Liu, W.L., Chen, W.J., 2013. Study of Pt catalyst on graphene and its application to fuel cell. Appl. Surf. Sci. 277, 223–230.

Jankauskaite, A., Vitkauskiene, A., Lazauskas, J., Baltrusaitis, I., Prosycevas, M., Andrulevicius, 2016. Bactericidal effect of graphene oxide/Cu/Ag nanoderivatives against Escherichia coli, Pseudomonas aeruginosa, Klebsiella pneumoniae, Staphylococcus aureus and Methicillin-resistant Staphylococcus aureus. Int. J. Pharm. 511 (1), 90–97.

Kahlert, Jan U., Rawal, Aditya, Hook, James M., Rendina, Louis M., Choucair, Mohammad, 2014.. Carborane functionalization of the aromatic network in chemically-synthesized graphene. Chem. Commun. 77.

Kaur, Prabhsharan, Shin, Mun-Sik, Joshi, Anjali, Kaur, Namarta, Sharma, Neha, Park, Jin-Soo, Sekhon, S.S., 2013. Interactions between multiwall carbon nanotubes and poly(diallyldimethylammonium) chloride: effect of the presence of a surfactant. J. Phys. Chem. B 117, 3161–3166.

Lazauskas, A., Baltrusaitis, J., Puodžiukynas, L., Andrulevičius, M., Bagdžiūnas, G., Volyniuk, D., Meškinis, Š., Niaura, G., Tamulevičius, T., Jankauskaitė, V., 2016. Characterization of urea derived polymeric carbon nitride and resultant thermally vacuum deposited amorphous thin films: Structural, chemical and photophysical properties. Carbon 107, 415–425.

Lei, M., Liang, C., Wang, Y.J., Huang, K., Ye, C.X., Liu, G., et al, 2013. Durable platinum/graphene catalysts assisted with polydiallyldimethylammonium for proton-exchange membrane fuel cells. Electrochim. Acta 113, 366e72.

Likai, W., Zhenghua, T., Wei, Y., Hongyu, Y., Qiannan, W., Shaowei, C., 2016. Porous carbon-supported gold nanoparticles for oxygen reduction reaction: effects of nanoparticle size. ACS Appl. Mater. Interfaces 8 (32), 20635–20641.

Lin, Y.-C., Lin, C.-Y., Chiu, P.-W., 2010. Controllable graphene N-doping with ammonia plasma. Appl. Phys. Lett. 96, No, 133110.

Liu, M., Zhang, R., Chen, W., 2014. Graphene-supported nanoelectrocatalysts for fuel cells: synthesis, properties, and applications. Chem. Rev. 114, 5117–5160.

Marinoiu, A., Raceanu, M., Carcadea, E., Pantazi, A., Mesterca, R., Tutunaru, O., Nica, S., Bala, D., Varlam, M., Enachescu, M., Synthesis of metal-dispersed nanoparticles on reduced graphene oxide and its application in PEM Fuel Cells, InTechOpen Book Chapter "Electrocatalysts", ISBN 978-953-51-6257-5.

Marinoiu, Adriana, Gatto, Irene, Raceanu, Mircea, Varlam, Mihai, Moise, Calin, Pantazi, Aida, Jianu, Catalin, Stefanescu, Ioan, Enachescu, Marius, 2017. Low cost iodine doped graphene for fuel cell electrodes. Int. J. Hydrogen Energy 42 (43), 26877–26888.

Marinoiu, Adriana, Jianu, Catalin, Cobzaru, Claudia, Raceanu, Mircea, Capris, Catalin, Soare, Amalia, Petreanu, Irina, Carcadea, Elena, 2017. Facile synthesis of well dispersed au nanoparticles on reduced graphene oxide. Progr. Cryogenics Isotopes Sep. 20 (2), 5–14.

Marinoiu, A., Teodorescu, C., Carcadea, E., Raceanu, M., Varlam, M., Cobzaru, C., Stefanescu, I., 2015. Graphene-based materials used as the catalyst support for PEMFC applications. Mater. Today: Proc. 2 (6), 3797–3805.

Marinoiu, A., Raceanu, M., Carcadea, E., Varlam, M., Stefanescu, I., 2016. Iodinated carbon materials for oxygen reduction reaction in proton exchange membrane fuel cell. Scalable synthesis and electrochemical performances. Arab. J. Chem.

Marinoiu, A., Raceanu, M., Carcadea, E., Varlam, M., Soare, A., Stefanescu, I., 2017. Doped graphene as non-metallic catalyst for fuel cells. Mater. Sci. (MEDŽIAGOTYRA) 23 (2), 108–113.

Marinoiu, A., Raceanu, M., Carcadea, E., Varlam, M., Stefanescu, I., 2017. Low cost iodine intercalated graphene for fuel cells electrodes. Appl. Surf. Sci. https://doi.org/10.1016/j.apsusc.2017.01.295.

Meier, C.J., Galeano, C., Katsounaros, I., Witte, J., Bongard, H.J., Topalov, A.A., et al, 2014. Design criteria for stable Pt/C fuel cell catalysts. Beilstein J. Nanotechnol. 5, 44–67.

NIST X-ray Photoelectron Spectroscopy Database, Version 3.5 (National Institute of Standards and Technology, Gaithersburg, 2003); http://srdata.nist.gov/xps/ (Accessed March 2, 2018).

Peng, Hongliang, Mo, Zaiyong, Liao, Shijun, Liang, Huagen, Yang, Lijun, Luo, Fan, Song, Huiyu, Zhong, Yiliang, Zhang, Bingqing, 1765. High performance Fe- and N-doped carbon catalyst with graphene structure for oxygen reduction. Sci. Reports 3. https://doi.org/10.1038/srep01765.

Proietti, Eric, Jaouen, Frédéric, Lefèvre, Michel, Larouche, Nicholas, Tian, Juan, Herranz, Juan, Dodelet, Jean-Pol, 2011. Iron-based cathode catalyst with enhanced power density in polymer electrolyte membrane fuel cells. Nat. Commun. 2 (416). https://doi.org/10.1038/ncomms1427.

Qiannan, W., Likai, W., Zhenghua, T., Fucai, W., Wei, Y., Hongyu, Y., Weijia, Z., Ligui, L., Xiongwu, K., Shaowei, C., 2016. Oxygen reduction catalyzed by gold nanoclusters supported on carbon nanosheets. Nanoscale 8, 6629–6635.

Shao, Y., Zhang, S., Wang, C., Nie, Z., Liu, J., Wang, Y., et al, 2010. Highly durable graphene nanoplatelets supported Pt nanocatalysts for oxygen reduction. J. Power Sources 195 (15), 4600–4605.

Song, Jenn-Ming, Pai, Tsung-Yun, Hsieh, Kun-Hung, Lai, Ming-Yan, Cheng, Chi-Nan, Liang, Sin-Yong, Lee, Hsin-Yi, Chen, Lung-Tai, 2016. Kinetic study on low temperature coalescence of carboxylate-protected Ag nanoparticles for interconnect applications. RSC Adv. 6, 97449.

Stolbov, Sergey, Alcántara Ortigoza, Marisol, 2015. Gold-doped graphene: a highly stable and active electrocatalysts for the oxygen reduction reaction. J. Chem. Phys. 142, 154703.

Tang, Z., Wu, W., Wang, K., 2018. Oxygen reduction reaction catalyzed by noble metal clusters. Catalysts 8, 65.

Tang, Yanan, Yang, Zongxian, Dai, Xianqi, 2011. Trapping of metal atoms in the defects on graphene. J. Chem. Phys. 135, 224704.

Vinayan, B.P., Diemant, T., Xiu-Mei, Lin, Cambaz, M.A., Golla-Schindler, U., Kaiser, U., Behm, R.J., Fichtner, M., 2016. Nitrogen rich hierarchically organized porous carbon/sulfur composite cathode electrode for high performance Li/S battery: a mechanistic investigation by operando spectroscopic studies. Adv. Mater. Interfaces 3, 1600372.

Wang, Li, Wang, Yi, Li, An, Yang, Yunshang, Tang, Qinghu, Cao, Hongbin, Qi, Tao, Li, Changming, July 2014. Electrocatalysis of carbon black- or poly(diallyldimethylammonium chloride)-functionalized activated carbon nanotubes-supported Pd-Tb towards methanol oxidation in alkaline media. J. Power Sources 257 (1), 138–146.

Wang, Shuangyin, Yu, Dingshan, Dai, Liming, Chang, Dong Wook, Baek, Jong-Beom, 2011. Polyelectrolyte-functionalized graphene a metal-free electrocatalysts for oxygen reduction. ACS Nano 5 (8), 6202–6209.

Wang, Shuangyin, Yu, Dingshan, Dai, Liming, 2011. Polyelectrolyte functionalized carbon nanotubes as efficient metal-free electrocatalysts for oxygen reduction. J. Am. Chem. Soc. 133 (14), 5182–5185.

Yaldagard, M., Jahanshahi, M., Seghatoleslami, N., 2013. Carbonaceous nanostructured support materials for low temperature fuel cell electrocatalysts e a review. World J. Nano Sci. Eng. 03, 121–153.

Yang, De-Quan, Rochette, Jean-Francois, Sacher, Edward, 2005. Spectroscopic evidence for π–π interaction between poly(diallyl dimethylammonium) chloride and multiwalled carbon nanotubes. J. Phys. Chem. B 109, 4481–4484.

Zhang, Bingyan, Huang, Dekang, Xiaobao, Xu., Alemu, Getachew, Zhang, Yibo, Zhan, Fang, Shen, Yan, Wang, Mingkui, 2013. Simultaneous electrochemical determination of ascorbic acid, dopamine and uric acid with helical carbon nanotubes. Electrochim. Acta 91, 261–266.

Please cite this article in press as: Marinoiu, A. et al., Low-cost preparation method of well dispersed gold nanoparticles on reduced graphene oxide and electrocatalytic stability in PEM fuel cell. Arabian Journal of Chemistry (2019), https://doi.org/10.1016/j.arabjc.2018.12.009